2-D Cooling and Trapping of a 2 Level Atom in a Rotating Cavity

Yusuf Kayra Gül[1,*]
[1] *Bilkent University, Department of Physics*
Universität Innsbruck, Institut für Theoretische Physik
(Dated: August 12, 2026)

Cooling and trapping time dynamics of a single 2 level atom in a rotating cavity or equivalently under Artificial Gauge Field has studied. Fully quantum mechanical model has constructed using 3 highly coupled harmonic oscillators corresponding to electromagnetic cavity field, and x and y mode of atom. Time dynamics of the excitations in the fields has simulated. Semiclassical model has constructed using Ehrenfest Theorem for cavity field intensity, and canonical position and momentum for x and y modes. In order to adress the first order quantum correlations, stochastic noise has introduced to the semiclassical equations. Time dynamics for cooling and trapping, and stationary state analysis has done for semiclassical approach.

I. MODEL

One can start with the general Jaynes–Cummings Hamiltonian in two dimensions for a two-level atom with a transverse pump in the z direction and a symmetric harmonic trapping potential after the rotating wave approximation and transformation to the pump frame:

$$\hat{H}_p = \hat{H}_{\text{cm}} + \hat{H}_{\text{cav}} + \hat{H}_{\text{at}} + \hat{H}_{\text{int}} + \hat{H}_{\text{pump}} \tag{1}$$

Here,

$$\hat{H}_{\text{cm}} = \frac{\hat{p}_x^2 + \hat{p}_y^2}{2m} + \frac{1}{2} m\omega_{\text{trap}}^2 \hat{r}^2 \tag{2}$$

$$\hat{H}_{\text{cav}} = -\hbar\Delta_c \hat{a}^\dagger \hat{a} \tag{3}$$

$$\hat{H}_{\text{at}} = -\hbar\Delta_a \hat{\sigma}_+ \hat{\sigma}_- \tag{4}$$

$$\hat{H}_{\text{int}} = -i\hbar g f_c \left(\hat{a}\hat{\sigma}_+ - \hat{a}^\dagger \hat{\sigma}_-\right) \tag{5}$$

$$\hat{H}_{\text{pump}} = \hbar\Omega_p \left(\hat{\sigma}_+ e^{ik_p z} + \hat{\sigma}_- e^{-ik_p z}\right) \tag{6}$$

Here $f_c = f_c(\hat{x}, \hat{y})$. The detunings are

$$\Delta_c = \omega_p - \omega_c \qquad \Delta_a = \omega_p - \omega_a \tag{7}$$

The corresponding Liouvillian is

$$\mathcal{L}\hat{\rho} = -\frac{i}{\hbar}[\hat{H}_p, \hat{\rho}] + \mathcal{D}_c\hat{\rho} + \mathcal{D}_a\hat{\rho} \tag{8}$$

with

$$\mathcal{D}_c\hat{\rho} = \kappa \left(2\hat{a}\hat{\rho}\hat{a}^\dagger - \hat{a}^\dagger\hat{a}\hat{\rho} - \hat{\rho}\hat{a}^\dagger\hat{a}\right) \tag{9}$$

$$\mathcal{D}_a\hat{\rho} = \Gamma \left(2\hat{\sigma}_-\hat{\rho}\hat{\sigma}_+ - \hat{\sigma}_+\hat{\sigma}_-\hat{\rho} - \hat{\rho}\hat{\sigma}_+\hat{\sigma}_-\right) \tag{10}$$

Setting $k_p z = 3\pi/2$, which is an arbitrary phase choice, the pump term becomes

$$\hat{H}_{\text{pump}} = -i\hbar\Omega_p \left(\hat{\sigma}_+ - \hat{\sigma}_-\right) \tag{11}$$

* kayra.gul@ug.bilkent.edu.tr

In the far-detuned or dispersive region,

$$|\Delta_a| \gg g, \kappa, \Omega_p \Gamma \tag{12}$$

the upper atomic state can be adiabatically eliminated. Thus,

$$\dot{\hat{\sigma}}_- \simeq 0 \qquad \hat{\sigma}_z \simeq -1 \tag{13}$$

Substituting the terms from Eq. (13) to the differential equation one can get considering Eq. (60) for $\hat{\sigma}_-$ operator the steady-state atomic operators can be found as,

$$\hat{\sigma}_- \simeq -\frac{g f_c \hat{a} + \Omega_p}{\Gamma - i\Delta_a} \tag{14}$$

and $(\hat{\sigma}_-)^\dagger = \hat{\sigma}_+$. The dispersive light shift, scattering rate, and effective pump strength are

$$U_0 = \frac{\Delta_a g^2}{\Delta_a^2 + \Gamma^2} \qquad \Gamma_0 = \frac{\Gamma g^2}{\Delta_a^2 + \Gamma^2}$$
$$\eta_{\text{eff}} = \frac{\Delta_a g \Omega_p}{\Delta_a^2 + \Gamma^2} \tag{15}$$

After adiabatic elimination, the effective Hamiltonian is

$$\hat{H}_{\text{eff}} = \hat{H}_{\text{cm}} - \hbar\Delta_{\text{eff}}\hat{a}^\dagger\hat{a} + \hbar\eta_{\text{eff}} f_c \left(\hat{a} + \hat{a}^\dagger\right) \tag{16}$$

Where the position-dependent effective detuning provides the energy shift of the cavity field as

$$\Delta_{\text{eff}}(\hat{x}, \hat{y}) = \Delta_c - U_0 f_c^2(\hat{x}, \hat{y}) \tag{17}$$

The effective Lindblad dissipator is

$$\mathcal{D}_{\text{eff}}\hat{\rho} = \left[\kappa + \Gamma_0 f_c^2(\hat{x}, \hat{y})\right] \left(2\hat{a}\hat{\rho}\hat{a}^\dagger - \hat{a}^\dagger\hat{a}\hat{\rho} - \hat{\rho}\hat{a}^\dagger\hat{a}\right) \tag{18}$$

The time evolution in the non-rotating pump frame is

$$i\hbar\partial_t |\psi(t)\rangle = \hat{H}_{\text{eff}} |\psi(t)\rangle \tag{19}$$

We transform to a frame rotating around the z axis with angular frequency Ω_{rot}. The angular momentum operator is

$$\hat{L}_z = \hat{x}\hat{p}_y - \hat{y}\hat{p}_x \tag{20}$$

The corresponding rotation operator is

$$\hat{R}_z(t) = \exp\left[-\frac{i}{\hbar}\Omega_{\rm rot}\hat{L}_z t\right] \tag{21}$$

The non-rotating and rotating states are related by

$$|\psi(t)\rangle = \hat{R}_z(t)\,|\psi_\Omega(t)\rangle \tag{22}$$

Substitution into Eq. (19) gives

$$i\hbar\partial_t\left[\hat{R}_z(t)\,|\psi_\Omega(t)\rangle\right] = \hat{H}_{\rm eff}\hat{R}_z(t)\,|\psi_\Omega(t)\rangle \tag{23}$$

Expanding the time derivative gives

$$i\hbar\left(\dot{\hat{R}}_z\,|\psi_\Omega\rangle + \hat{R}_z\partial_t\,|\psi_\Omega\rangle\right) = \hat{H}_{\rm eff}\hat{R}_z\,|\psi_\Omega\rangle \tag{24}$$

Multiplying by $\hat{R}_z^\dagger$ from the left,

$$i\hbar\partial_t\,|\psi_\Omega\rangle = \left(\hat{R}_z^\dagger\hat{H}_{\rm eff}\hat{R}_z - i\hbar\hat{R}_z^\dagger\dot{\hat{R}}_z\right)|\psi_\Omega\rangle \tag{25}$$

Therefore, the rotating-frame Hamiltonian is

$$\hat{H}_\Omega = \hat{R}_z^\dagger\hat{H}_{\rm eff}\hat{R}_z - i\hbar\hat{R}_z^\dagger\dot{\hat{R}}_z \tag{26}$$

Since

$$\dot{\hat{R}}_z = -\frac{i}{\hbar}\Omega_{\rm rot}\hat{L}_z\hat{R}_z \tag{27}$$

we obtain

$$-i\hbar\hat{R}_z^\dagger\dot{\hat{R}}_z = -\Omega_{\rm rot}\hat{L}_z \tag{28}$$

Thus,

$$\hat{H}_\Omega = \hat{R}_z^\dagger\hat{H}_{\rm eff}\hat{R}_z - \Omega_{\rm rot}\hat{L}_z \tag{29}$$

The coordinate and momentum transformations are written compactly as

$$\hat{\mathbf{r}}_{\rm lab} = R(\Omega_{\rm rot}t)\hat{\mathbf{r}} \qquad \hat{\mathbf{p}}_{\rm lab} = R(\Omega_{\rm rot}t)\hat{\mathbf{p}} \tag{30}$$

where

$$R(\theta) = \begin{pmatrix}\cos\theta & -\sin\theta\\ \sin\theta & \cos\theta\end{pmatrix} \tag{31}$$

Since the trap is symmetric,

$$\hat{R}_z^\dagger\hat{H}_{\rm cm}\hat{R}_z = \hat{H}_{\rm cm} \tag{32}$$

The rotation term can be represented using a synthetic vector potential,

$$\hat{\mathbf{A}}_\Omega = m\Omega_{\rm rot}\left(-\hat{y}\,\hat{\mathbf{x}} + \hat{x}\,\hat{\mathbf{y}}\right) \tag{33}$$

Then the rotating-frame Hamiltonian becomes

$$\begin{aligned}\hat{H}_\Omega = {}& \frac{\left(\hat{\mathbf{p}} - \hat{\mathbf{A}}_\Omega\right)^2}{2m} + \frac{1}{2}m\omega_{\rm trap}^2\hat{r}^2 + \hat{W}_{\rm rot}\\ & - \hbar\Delta_{\rm eff}\hat{a}^\dagger\hat{a} + \hbar\eta_{\rm eff}f_c\left(\hat{a} + \hat{a}^\dagger\right)\end{aligned} \tag{34}$$

where

$$\hat{W}_{\rm rot} = -\frac{1}{2}m\Omega_{\rm rot}^2\hat{r}^2 \tag{35}$$

In this work, an additional harmonic trapping potential is introduced to exactly compensate the centrifugal anti-trapping term:

$$\hat{V}_{\rm comp} = +\frac{1}{2}m\Omega_{\rm rot}^2\hat{r}^2 \tag{36}$$

Therefore,

$$\hat{W}_{\rm rot} + \hat{V}_{\rm comp} = 0 \tag{37}$$

The final compensated rotating-frame Hamiltonian is

$$\begin{aligned}\hat{H}_\Omega^{\rm (comp)} = {}& \frac{\left(\hat{\mathbf{p}} - \hat{\mathbf{A}}_\Omega\right)^2}{2m} + \frac{1}{2}m\omega_{\rm trap}^2\hat{r}^2\\ & - \hbar\Delta_{\rm eff}\hat{a}^\dagger\hat{a} + \hbar\eta_{\rm eff}f_c\left(\hat{a} + \hat{a}^\dagger\right)\end{aligned} \tag{38}$$

We assume that the cavity mode is fixed in the rotating frame, so that the spatial mode function remains time independent after the transformation. We choose

$$f_c(\hat{x},\hat{y}) = \cos(k\hat{x}) \tag{39}$$

and remove the subscript from the vector potential for simplicity:

$$\hat{\mathbf{A}} = m\Omega_{\rm rot}\left(-\hat{y}\,\hat{\mathbf{x}} + \hat{x}\,\hat{\mathbf{y}}\right) \tag{40}$$

Therefore, the final Hamiltonian reads

$$\begin{aligned}\hat{H} = {}& \frac{\left(\hat{\mathbf{p}} - \hat{\mathbf{A}}\right)^2}{2m} + \frac{1}{2}m\omega_{\rm trap}^2\hat{r}^2\\ & - \hbar\left[\Delta_c - U_0\cos^2(k\hat{x})\right]\hat{a}^\dagger\hat{a}\\ & + \hbar\eta_{\rm eff}\cos(k\hat{x})\left(\hat{a} + \hat{a}^\dagger\right)\end{aligned} \tag{41}$$

and the Lindblad dissipator is,

$$\mathcal{D}_{\rm eff}\hat{\rho} = \left[\kappa + \Gamma_0\cos^2(k\hat{x})\right]\left(2\hat{a}\hat{\rho}\hat{a}^\dagger - \hat{a}^\dagger\hat{a}\hat{\rho} - \hat{\rho}\hat{a}^\dagger\hat{a}\right) \tag{42}$$

A. Quantum Harmonic Oscillator Approach

One can rewrite the final Hamiltonian in Eq. (41) by distributing the vector potential, $\hat{\mathbf{A}}$. After algebraic manipulations the Hamiltonian reads,

$$\begin{aligned}\hat{H} = {}& \frac{\hat{p}^2}{2m} + \frac{1}{2}m\left(\Omega_{\rm rot}^2 + \omega_{\rm trap}^2\right)\hat{r}^2\\ & - \Omega_{\rm rot}\left(\hat{p}_y\hat{x} - \hat{p}_x\hat{y}\right)\\ & - \hbar\left(\Delta_c - U_0\cos^2(k\hat{x})\right)\hat{a}^\dagger\hat{a}\end{aligned}$$

$$+ \hbar\eta_{\text{eff}}\left(\hat{a}^\dagger + \hat{a}\right)\cos(k\hat{x}) \tag{43}$$

After substituting $\hat{p}^2 = \hat{p}_x^2 + \hat{p}_y^2$, $\hat{r}^2 = \hat{x}^2 + \hat{y}^2$ and $\omega_o = \sqrt{\Omega_{\text{rot}}^2 + \omega_{\text{trap}}^2}$ Hamiltonian converts into,

$$\begin{aligned}\hat{H} &= \left[\frac{\hat{p}_x^2}{2m} + \frac{1}{2}m\omega_o^2\hat{x}^2\right] + \left[\frac{\hat{p}_y^2}{2m} + \frac{1}{2}m\omega_o^2\hat{y}^2\right] \\ &- \Omega_{\text{rot}}\left(\hat{p}_y\hat{x} - \hat{p}_x\hat{y}\right) \\ &- \hbar\left(\Delta_c - U_0\cos^2(k\hat{x})\right)\hat{a}^\dagger\hat{a} \\ &+ \hbar\eta_{\text{eff}}\left(\hat{a}^\dagger + \hat{a}\right)\cos(k\hat{x})\end{aligned} \tag{44}$$

As it can be seen from Eq. (44), one can define harmonic oscillator creation and annihilation operators for x and y directions. The mentioned operators are defined as:

$$\begin{aligned}\hat{b}_x &= \sqrt{\frac{m\omega_o}{2\hbar}}\left(\hat{x} + \frac{i}{m\omega_o}\hat{p}_x\right) \\ \hat{b}_y &= \sqrt{\frac{m\omega_o}{2\hbar}}\left(\hat{y} + \frac{i}{m\omega_o}\hat{p}_y\right)\end{aligned} \tag{45}$$

Therefore x operator reads,

$$\hat{x} = \sqrt{\frac{\hbar}{2m\omega_o}}\left(\hat{b}_x^\dagger + \hat{b}_x\right) \tag{46}$$

Via substituting Eqs. (45) and (46) to Eq. (44) Hamiltonian can be rewritten as,

$$\begin{aligned}\hat{H} &= \hbar\omega_o\left(\hat{b}_x^\dagger\hat{b}_x + \frac{1}{2}\right) + \hbar\omega_o\left(\hat{b}_y^\dagger\hat{b}_y + \frac{1}{2}\right) \\ &- \hbar\left(\Delta_c - U_0\cos^2\left[\sqrt{\frac{\omega_r}{\omega_o}}\left(\hat{b}_x^\dagger + \hat{b}_x\right)\right]\right)\hat{a}^\dagger\hat{a} \\ &- i\hbar\Omega_{\text{rot}}\left(\hat{b}_x\hat{b}_y^\dagger - \hat{b}_x^\dagger\hat{b}_y\right) \\ &+ \hbar\eta_{\text{eff}}\left(\hat{a}^\dagger + \hat{a}\right)\cos\left[\sqrt{\frac{\omega_r}{\omega_o}}\left(\hat{b}_x^\dagger + \hat{b}_x\right)\right]\end{aligned} \tag{47}$$

where $\omega_r = \hbar k^2/2m$. One can also rewrite the Lindblad dissipator by substituting ladder operator representation of x into Eq. (18),

$$\begin{aligned}\mathcal{D}_{\text{eff}}\hat{\rho} &= \left[\kappa + \Gamma_0\cos^2\left[\sqrt{\frac{\omega_r}{\omega_o}}\left(\hat{b}_x^\dagger + \hat{b}_x\right)\right]\right] \\ &\times\left(2\hat{a}\hat{\rho}\hat{a}^\dagger - \hat{a}^\dagger\hat{a}\hat{\rho} - \hat{\rho}\hat{a}^\dagger\hat{a}\right)\end{aligned} \tag{48}$$

This approach allows us to consider the system as three highly coupled quantum harmonic oscillators.

Analytical Idea 1 - We can perturbatively solve the energy shifts of eigenstates due to term with U_0 and η_{eff} and observe what happens in the weak pump and far detuning regime.

B. Stationary State Analysis for Quantum Harmonic Oscillator Approach

For the quantum harmonic oscillator approach, the Hamiltonian and dissipator are

$$\begin{aligned}\hat{H} &= \hbar\omega_o\left(\hat{b}_x^\dagger\hat{b}_x + \frac{1}{2}\right) + \hbar\omega_o\left(\hat{b}_y^\dagger\hat{b}_y + \frac{1}{2}\right) \\ &- \hbar\left(\Delta_c - U_0\cos^2\left[\sqrt{\frac{\omega_r}{\omega_o}}\left(\hat{b}_x^\dagger + \hat{b}_x\right)\right]\right)\hat{a}^\dagger\hat{a} \\ &- i\hbar\Omega_{\text{rot}}\left(\hat{b}_x\hat{b}_y^\dagger - \hat{b}_x^\dagger\hat{b}_y\right) \\ &+ \hbar\eta_{\text{eff}}\left(\hat{a}^\dagger + \hat{a}\right)\cos\left[\sqrt{\frac{\omega_r}{\omega_o}}\left(\hat{b}_x^\dagger + \hat{b}_x\right)\right]\end{aligned} \tag{49}$$

and

$$\begin{aligned}\mathcal{D}\hat{\rho} &= \left[\kappa + \Gamma_0\cos^2\left[\sqrt{\frac{\omega_r}{\omega_o}}\left(\hat{b}_x^\dagger + \hat{b}_x\right)\right]\right] \\ &\times\left(2\hat{a}\hat{\rho}\hat{a}^\dagger - \hat{a}^\dagger\hat{a}\hat{\rho} - \hat{\rho}\hat{a}^\dagger\hat{a}\right)\end{aligned} \tag{50}$$

where

$$\omega_r = \frac{\hbar k^2}{2m} \qquad \omega_o = \sqrt{\Omega_{\text{rot}}^2 + \omega_{\text{trap}}^2} \tag{51}$$

and

$$U_0 = \frac{\Delta_a g^2}{\Delta_a^2 + \Gamma^2} \qquad \Gamma_0 = \frac{\Gamma g^2}{\Delta_a^2 + \Gamma^2} \qquad \eta_{\text{eff}} = \frac{\Delta_a g\Omega_p}{\Delta_a^2 + \Gamma^2} \tag{52}$$

The master equation is

$$\frac{d\hat{\rho}}{dt} = \frac{i}{\hbar}\left[\hat{\rho}, \hat{H}\right] + \mathcal{D}\hat{\rho} = \mathcal{L}\left(\hat{\rho}\right) \tag{53}$$

To find the stationary state of the quantum system, we solve

$$\mathcal{L}\left(\hat{\rho}\right) = 0 \tag{54}$$

For compact notation, we define

$$\hat{X} = \sqrt{\frac{\omega_r}{\omega_o}}\left(\hat{b}_x^\dagger + \hat{b}_x\right) \tag{55}$$

$$\hat{C} = \cos\left(\hat{X}\right) \tag{56}$$

$$\hat{n}_c = \hat{a}^\dagger\hat{a} \qquad \hat{n}_x = \hat{b}_x^\dagger\hat{b}_x \qquad \hat{n}_y = \hat{b}_y^\dagger\hat{b}_y \tag{57}$$

$$\hat{K} = \hat{b}_x\hat{b}_y^\dagger - \hat{b}_x^\dagger\hat{b}_y \tag{58}$$

Then the stationary Liouvillian equation can be written explicitly as

$$\begin{aligned}\mathcal{L}\left(\hat{\rho}\right) = i\omega_o &\left[\left(\hat{\rho}\hat{n}_x - \hat{n}_x\hat{\rho}\right) + \left(\hat{\rho}\hat{n}_y - \hat{n}_y\hat{\rho}\right)\right] \\ &- i\Delta_c\left(\hat{\rho}\hat{n}_c - \hat{n}_c\hat{\rho}\right) \\ &+ iU_0\left(\hat{\rho}\hat{C}^2\hat{n}_c - \hat{C}^2\hat{n}_c\hat{\rho}\right) \\ &+ \Omega_{\text{rot}}\left[\hat{\rho}\hat{K} - \hat{K}\hat{\rho}\right]\end{aligned}$$

$$+ i\eta_{\text{eff}} \left[\hat{\rho}\left(\hat{a}^\dagger + \hat{a}\right)\hat{C} - \left(\hat{a}^\dagger + \hat{a}\right)\hat{C}\hat{\rho}\right] + \left[\kappa + \Gamma_0 \hat{C}^2\right]\left(2\hat{a}\hat{\rho}\hat{a}^\dagger - \hat{a}^\dagger\hat{a}\hat{\rho} - \hat{\rho}\hat{a}^\dagger\hat{a}\right) = 0 \quad (59)$$

This linear equation can be solved for $\hat{\rho}$ to find the steady states of the system.

C. Semi-Classical Approach

One can use Ehrenfest Theorem to consider operators as numbers in a semiclassical point of view. The Ehrenfest formula reads as,

$$\frac{d}{dt}\langle\hat{O}\rangle = \frac{i}{\hbar}\left\langle\left[\hat{H}, \hat{O}\right]\right\rangle + \sum_j \left\langle\mathcal{L}_j^\dagger[\hat{O}]\right\rangle + \left\langle\frac{\partial\hat{O}}{\partial t}\right\rangle \quad (60)$$

Where $\hat{O}$ denotes any arbitrary operator and $\text{Tr}\left[(\mathcal{L}\hat{\rho})\hat{O}\right] = \text{Tr}\left[\hat{\rho}(\mathcal{L}^\dagger\hat{O})\right]$. We can say that the operators do not have any explicit time dependence so $\partial_t\hat{O} = 0$ in general.

One can define $\alpha = \langle a\rangle$ which is an approximation assuming relatively high photon number and $\alpha = \alpha_R + i\alpha_I$ for the sake of semiclassical approximation. By using Eq. (41) in Eq. (60) one can derive a set of differential equations describing the system as follows,

$$\frac{dx}{dt} = \frac{p_x}{m} + \Omega_{\text{rot}}y, \qquad \frac{dy}{dt} = \frac{p_y}{m} - \Omega_{\text{rot}}x \quad (61a)$$

$$\frac{dp_x}{dt} = \hbar U_0 k|\alpha|^2\sin(2kx) + 2\hbar\eta_{\text{eff}}k\alpha_R\sin(kx) + \Omega_{\text{rot}}p_y - \omega_o^2 mx + \xi_{p_x} \quad (61b)$$

$$\frac{dp_y}{dt} = -\Omega_{\text{rot}}p_x - \omega_o^2 my + \xi_{p_y} \quad (61c)$$

$$\frac{d\alpha_R}{dt} = -\left[\kappa + \Gamma_0\cos^2(kx)\right]\alpha_R - \left[\Delta_c - U_0\cos^2(kx)\right]\alpha_I + \xi_{\alpha_R} \quad (61d)$$

$$\frac{d\alpha_I}{dt} = -\left[\kappa + \Gamma_0\cos^2(kx)\right]\alpha_I + \left[\Delta_c - U_0\cos^2(kx)\right]\alpha_R - \eta_{\text{eff}}\cos(kx) + \xi_{\alpha_I} \quad (61e)$$

Where ξ_i are Langevin noise terms originating from vacuum field input and spontaneous emission of the atom with corresponding correlation functions,

$$\langle\xi_{\alpha_R}\xi_{\alpha_R}\rangle = \langle\xi_{\alpha_I}\xi_{\alpha_I}\rangle = \frac{1}{2}\left[\kappa + \Gamma_0\cos^2(kx)\right] \quad (62a)$$

$$\langle\xi_{p_x}\xi_{\alpha_R}\rangle = \hbar k\Gamma_0\sin(2kx)\alpha_I \quad (62b)$$

$$\langle\xi_{p_x}\xi_{\alpha_I}\rangle = -\hbar k\Gamma_0\sin(2kx)\alpha_R \quad (62c)$$

$$\langle\xi_{p_x}\xi_{p_x}\rangle = 2\hbar^2k^2\Gamma_0|\alpha|^2\left(\cos^2(kx)\bar{u}_x^2 + \sin^2(kx)\right) \quad (62d)$$

$$\left\langle\xi_{p_y}\xi_{p_y}\right\rangle = 2\hbar^2k^2\Gamma_0|\alpha|^2\cos^2(kx)\bar{u}_y^2 \quad (62e)$$

Where $\bar{u}_i$ are the averaged projection of the spontaneous emission on corresponding axes.

The Langevin equation can be written in differential form as

$$d\mathbf{u} = \mathbf{F}(\mathbf{u})dt + \mathbf{B}(\mathbf{u})d\mathbf{W} \quad (63)$$

Here $\mathbf{u} = (x, y, p_x, p_y, \alpha_R, \alpha_I)^T$ and $d\mathbf{W}$ is a Wiener increment. The number of independent Wiener increments is chosen such that the matrix $\mathbf{B}$ satisfies following relation to diffusion matrix $\mathbf{D}$,

$$\mathbf{D} = \mathbf{B}\mathbf{B}^T \quad (64)$$

and the noise correlations satisfy

$$\langle dW_i dW_j\rangle = \delta_{ij}dt \qquad \langle\xi_i(t)\xi_j(t')\rangle = D_{ij}\delta(t-t') \quad (65)$$

These relations provide a convenient way to convert the Langevin equations into Wiener process form, which is more suitable for numerical implementation.

The canonical momenta in the rotating frame are not directly equal to the mechanical momenta. This distinction follows from the position equations in Eq. (61),

$$\dot{x} = \frac{p_x}{m} + \Omega_{\text{rot}}y \qquad \dot{y} = \frac{p_y}{m} - \Omega_{\text{rot}}x \quad (66)$$

which imply the velocity-related mechanical momenta

$$p_{x,\text{mech}} = m\dot{x} = p_x + m\Omega_{\text{rot}}y \quad (67)$$

$$p_{y,\text{mech}} = m\dot{y} = p_y - m\Omega_{\text{rot}}x \quad (68)$$

Therefore, the canonical and mechanical kinetic energies are different:

$$E_{\text{canonical}} = \frac{p_x^2 + p_y^2}{2m} \quad (69)$$

$$E_{\text{mechanical}} = \frac{p_{x,\text{mech}}^2 + p_{y,\text{mech}}^2}{2m} \quad (70)$$

The mechanical kinetic energy is the more physical cooling diagnostic, since it is connected to the actual velocity of the particle in the rotating frame.

D. Stationary State Analysis for Semiclassical Approach

One can neglect Langevin noise terms in set of stochastic differential equations Eq. (61), which allows them to be considered as ordinary differential equations.

To find the stationary states of the system some assumptions are needed. If there were no rotation transverse position and momentum would not be coupled so the motion on y direction would simply be a simple harmonic motion around $y = 0$. When rotation introduced equation got coupled and hard to foresee but one can assume that the mean y throughout the motion will be

$y = 0$ since there is no optical extrema along y direction other than the minimum point of trapping potential. Therefore one can say $y_{\text{fix}} = 0$.

For the p_y one can assume that there will also be a mean value lets say $p_{y\text{fix}}$ which also will make a oscillation around a fixed value, keeping in the mind that oscillations can be damped or in a complex shape. Therefore one can also say $p_y = p_{y\text{fix}}$.

To find the steady states one can susbtitute $p_y = p_{y\text{fix}}$ and $y = y_{\text{fix}}$ without claiming that the time derivatives of p_y and y are zero. Then by setting the time derivatives for x, p_x, α_R and α_I to zero one can get the following set of equations.

$$\frac{p_x}{m} + \Omega_{\text{rot}} y_{\text{fix}} = 0 \tag{71a}$$

$$\begin{aligned}\hbar U_0 k|\alpha|^2 \sin(2kx) + 2\hbar\eta_{\text{eff}} k\alpha_R \sin(kx)\\ + \Omega_{\text{rot}} p_{y\text{fix}} - \omega_o^2 m x = 0\end{aligned} \tag{71b}$$

$$-\kappa_{\text{eff}}\alpha_R - \Delta_{\text{eff}}\alpha_I = 0 \tag{71c}$$

$$-\kappa_{\text{eff}}\alpha_I + \Delta_{\text{eff}}\alpha_R - \eta_{\text{eff}}\cos(kx) = 0 \tag{71d}$$

Where $\kappa_{\text{eff}} = \kappa + \Gamma_0 \cos^2(kx)$ and $\Delta_{\text{eff}} = \Delta_c - U_0 \cos^2(kx)$. One can see from Eq. (71a) that in steady state $p_{x_{ss}} = -m\Omega_{\text{rot}} y_{\text{fix}} = 0$, where ss denotes the steady state, since $y_{\text{fix}} = 0$. After a set of algebraic manipulations we get the equation for x_{ss} and $|\alpha|^2_{ss}$ as follows,

$$\frac{\hbar k \eta_{\text{eff}}^2 \Delta_c \sin(2kx_{ss})}{\kappa_{\text{eff}ss}^2 + \Delta_{\text{eff}ss}^2} = \omega_o^2 m x_{ss} - \Omega_{\text{rot}} p_{y\text{fix}} \tag{72}$$

$$|\alpha|^2_{ss} = \frac{\eta_{\text{eff}}^2 \cos^2(kx_{ss})}{\kappa_{\text{eff}ss}^2 + \Delta_{\text{eff}ss}^2} \tag{73}$$

Where $\omega_o = \sqrt{\Omega_{\text{rot}}^2 + \omega_{\text{trap}}^2}$. Eqs. (72) and (73) can be solved by root finding algorithms for an arbitrary set of parameters to find the steady states of the system.

The stability of the steady states can be determined by using Taylor Expansion and Jacobian analysis. One can start with the reduced vector of variables $\mathbf{v} = (x, p_x, \alpha_R, \alpha_I)^T$ since y and p_y are taken as parameters such that $y = y_{\text{fix}}$ and $p_y = p_{y\text{fix}}$. Then the system of ordinary differential equations can be written in the form,

$$\frac{\partial \mathbf{v}}{\partial t} = \mathbf{G}(\mathbf{v}) \tag{74}$$

Where $\mathbf{G}(\mathbf{v})$ denotes the system given in Eq. (61) but reduced for $\mathbf{v}$. Then for steady state vector $\mathbf{v}_{ss} = (x_{ss}, p_{x_{ss}}, \alpha_{R_{ss}}, \alpha_{I_{ss}})^T$ the condition is,

$$\frac{\partial \mathbf{v}_{ss}}{\partial t} = \mathbf{G}(\mathbf{v}_{ss}) = 0 \tag{75}$$

Then one can define $\delta\mathbf{v} = (\delta x, \delta p_x, \delta\alpha_R, \delta\alpha_I)^T$ to Taylor expand $\mathbf{G}(\mathbf{v})$ around $\mathbf{v}_{ss}$ by first considering $\mathbf{v} = \mathbf{v}_{ss} + \delta\mathbf{v}$ such that,

$$\begin{aligned}\frac{\partial}{\partial t}(\mathbf{v}_{ss} + \delta\mathbf{v}) &= \mathbf{G}(\mathbf{v}_{ss} + \delta\mathbf{v})\\ &= \mathbf{G}(\mathbf{v}_{ss}) + \mathbf{J}(\mathbf{v}_{ss})\delta\mathbf{v}\end{aligned} \tag{76}$$

where

$$\mathbf{J}(\mathbf{v}_{ss}) = \left.\frac{\partial \mathbf{G}}{\partial \mathbf{v}}\right|_{\mathbf{v}_{ss}} \tag{77}$$

Then, using the equality in Eq. (75),

$$\frac{\partial \delta\mathbf{v}}{\partial t} = \mathbf{J}(\mathbf{v}_{ss})\delta\mathbf{v} \tag{78}$$

Then the Jacobian matrix can be written compactly as

$$\mathbf{J}(\mathbf{v}_{ss}) = \left.\begin{pmatrix} 0 & \frac{1}{m} & 0 & 0\\ J_{21} & 0 & J_{23} & J_{24}\\ J_{31} & 0 & J_{33} & J_{34}\\ J_{41} & 0 & J_{43} & J_{44}\end{pmatrix}\right|_{\mathbf{v}_{ss}} \tag{79}$$

where

$$\begin{aligned}J_{21} = 2\hbar U_0 k^2 |\alpha|^2 \cos(2kx)\\ + 2\hbar\eta_{\text{eff}} k^2 \alpha_R \cos(kx) - m\omega_o^2\end{aligned} \tag{80a}$$

$$\begin{aligned}J_{23} = 2\hbar U_0 k\alpha_R \sin(2kx)\\ + 2\hbar\eta_{\text{eff}} k \sin(kx)\end{aligned} \tag{80b}$$

$$J_{24} = 2\hbar U_0 k\alpha_I \sin(2kx) \tag{80c}$$

$$\begin{aligned}J_{31} = \Gamma_0 k \sin(2kx)\alpha_R\\ - U_0 k \sin(2kx)\alpha_I\end{aligned} \tag{80d}$$

$$J_{33} = -\left[\kappa + \Gamma_0 \cos^2(kx)\right] \tag{80e}$$

$$J_{34} = -\left[\Delta_c - U_0 \cos^2(kx)\right] \tag{80f}$$

$$\begin{aligned}J_{41} = \Gamma_0 k \sin(2kx)\alpha_I\\ + U_0 k \sin(2kx)\alpha_R\\ + \eta_{\text{eff}} k \sin(kx)\end{aligned} \tag{80g}$$

$$J_{43} = \Delta_c - U_0 \cos^2(kx) \tag{80h}$$

$$J_{44} = -\left[\kappa + \Gamma_0 \cos^2(kx)\right] \tag{80i}$$

The steady state is stable if all real parts of the eigenvalues of $\mathbf{J}(\mathbf{v}_{ss})$ are negative

$$\text{Re}(\lambda_i) < 0 \qquad \forall i \tag{81}$$

Since it indicates that the solution for the variables will include an exponential term with negative exponent leading to a decay over time.

SS Analysis Idea 1 - Many trajectories can be simulated starting from random initial conditions and via increasing the Ω_{rot} we can calculate the statistics of steady states.

SS Analysis Idea 2 - We might not need Ω_{rot} term in steady state equations since it will still be present in the Jacobian and affect the stability. This assumes a steady state for full system but in some cases reduced system reaches the steady state while y direction stays oscillatory. So a combined numerical analysis can be used and to find $p_{y\text{fix}}$ simulation results can be used for each point acquired from the reduced system approach.

II. SIMULATION RESULTS

The dimensionless variables defined as $X = kx$, $Y = ky$, $P_x = p_x/\hbar k$, $P_y = p_y/\hbar k$, $\mathcal{E} = E/\hbar\omega_r$ and $\tau = \omega_r t$ where $\omega_r = \hbar k^2/2m$. In the numerical simulations all equations are reformulated and the results are plotted using mentioned dimensionless variables.

A. Quantum Harmonic Oscillator Approach

In this part the parameters are chosen as following unless they are specified otherwise,

$$\begin{gathered}\Gamma = 1\omega_r \quad g = 1\omega_r \quad \kappa = 1\omega_r \\ \Delta_c = -2\omega_r \quad \Delta_a = -200\omega_r \quad \eta_{\text{eff}} = 0.6\omega_r \\ \Omega_{\text{rot}} = 0.1\omega_r \quad \omega_{\text{trap}} = 0.5\omega_r\end{gathered} \tag{82}$$

First the dynamics of the system has studied. Initial state has chosen as $\psi_0 = |n_c, n_x, n_y\rangle$ where n_i corresponds to eigenstates of the each harmonic oscillator.

In order to see the effect of rotation on dynamics of the system two main cases with $\Omega_{\text{rot}} = 0\omega_r$ and $\Omega_{\text{rot}} = 0.1\omega_r$ has studied where the other parameters are specified in Eq. (82). For each case we used four different initial states to seek distinct steady states of the system.

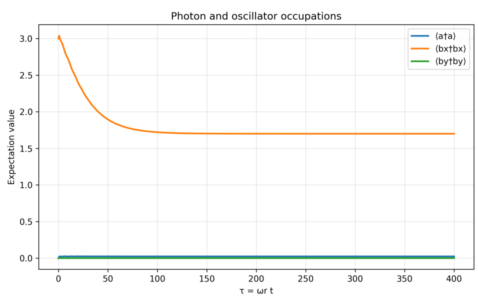

(a) $\Omega_{\text{rot}} = 0\omega_r$

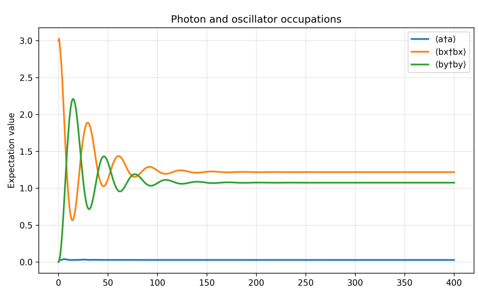

(b) $\Omega_{\text{rot}} = 0.1\omega_r$

FIG. 1. Quantum harmonic oscillator dynamics for the initial state $\psi_0 = |0, 3, 0\rangle$. All other parameters are chosen as in Eq. (82).

As it can be seen from Fig. 1 nearly no excitation in the cavity field has emerged for the both cases but still the energy of the particle decreased since the total expectation value of $b_x^\dagger b_x$ and $b_y^\dagger b_y$ is decreasing so we can say the particle cools down in the both cases. The figure also indicates a more effective cooling in x direction due to rotation but due to excitation in y direction the total energy is lower for the non-rotating case. Again as it can be seen from Fig. 2 nearly no excitation has emerged in both cases and we can see more efficient cooling in x direction in presence of rotation. Nevertheless, again due to excitations in y direction caused by rotation total energy is higher than the non-rotating case.

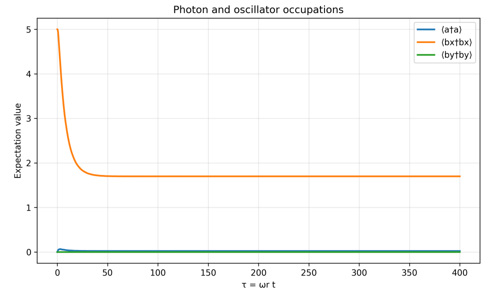

(a) $\Omega_{\text{rot}} = 0\omega_r$

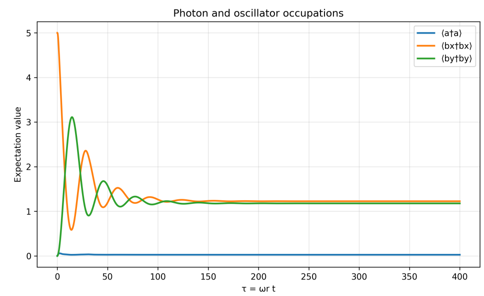

(b) $\Omega_{\text{rot}} = 0.1\omega_r$

FIG. 2. Quantum harmonic oscillator dynamics for the initial state $\psi_0 = |0, 5, 0\rangle$. All other parameters are chosen as in Eq. (82).

Therefore, we can investigate that if the particle start from a state that is both excited for x and y direction is it possible to cool it down more efficiently using rotation?

As it can be seen from Fig. 3 nearly no excitation in the cavity field has emerged in both cases similar to previous figures. Also the particle has cooled down more efficiently in rotating case for both direction eventually reaching even lower total energy than the non-rotating case. Interestingly, we can also observe that the steady state for the rotating case has changed due to different initial conditions but for non-rotating case has reached the same steady state as in the previous figures. Nevertheless, for non-rotating case the steady state for y direction is changing with the initial condition but we only consider x direction since y direction is completely decoupled when there is no rotation.

For Fig. 4 also nearly no cavity field has excited but the cooling in rotating case much more effective then non-rotating case. Again the system has reached one of the two observed steady states for the rotating case but the steady state in non-rotating case is the same as previous figures.

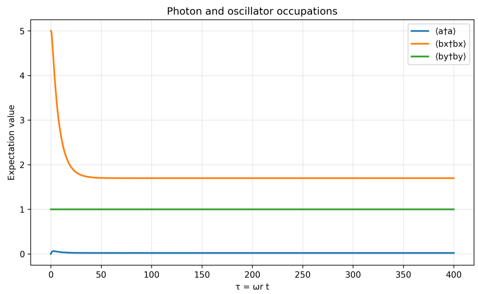

(a) $\Omega_{\rm rot} = 0\omega_r$

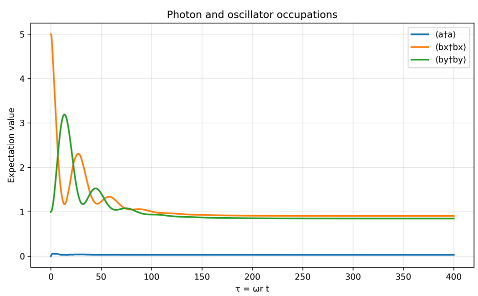

(b) $\Omega_{\rm rot} = 0.1\omega_r$

FIG. 3. Quantum harmonic oscillator dynamics for the initial state $\psi_0 = |0, 5, 1\rangle$. All other parameters are chosen as in Eq. (82).

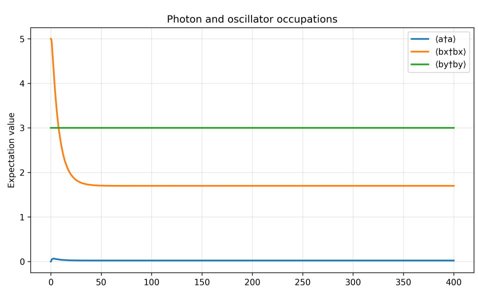

(a) $\Omega_{\rm rot} = 0\omega_r$

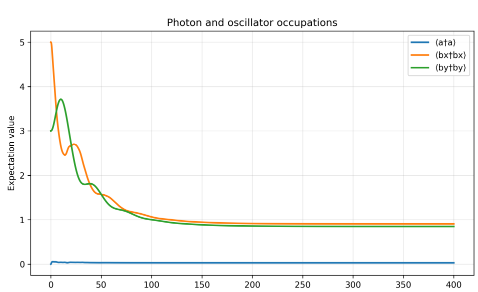

(b) $\Omega_{\rm rot} = 0.1\omega_r$

FIG. 4. Quantum harmonic oscillator dynamics for the initial state $\psi_0 = |0, 5, 3\rangle$. All other parameters are chosen as in Eq. (82).

Plot Idea 1 - We can also investigate the evolution of eigenstates and corresponding eigenenergies with increasing $\Omega_{\rm rot}$ for other parameters fixed or with increasing $\eta_{\rm eff}$ for other parameters fixed.

Plot Idea 2 - We can investigate different steady states via starting from different initial conditions. For example initial n_x on one axis and n_y on another axis then the points show the final $n_x, n_y, |\alpha|^2$ for those corresponding initial states.

B. Semi-Classical Approach

The main observation we got from fully quantum mechanical model was the cooling of transverse direction due to presence of rotation.

We will investigate the semi-classical model to make the same observation. Nevertheless, we cannot use the exact parameters that is used in Eq. (82) because the definition $\alpha = \langle a \rangle$ depends on relatively high photon number present in the cavity at steady state. Therefore, chosen parameters for this model are as follows unless they are specified otherwise,

$$\begin{gathered} \Gamma = 1\omega_r \quad g = 1\omega_r \quad \kappa = 1\omega_r \\ \Delta_c = -1\omega_r \quad \Delta_a = -200\omega_r \quad \eta_{\rm eff} = 2\omega_r \\ \Omega_{\rm rot} = 1\omega_r \quad \omega_{\rm trap} = 0.5\omega_r \end{gathered} \tag{83}$$

Initial state has chosen as $\mathbf{u_0} = (x_0, y_0, p_{x_0}, p_{y_0}, \alpha_{R_0}, \alpha_{I_0})$.In order to see the effect of rotation on dynamics of the system two main cases with $\Omega_{\rm rot} = 0\omega_r$ and $\Omega_{\rm rot} = 1\omega_r$ has studied where the other parameters are specified in Eq. (83). For each case we used four different initial states to seek distinct steady states of the system.

First the case with no noise will be studied with relatively high initial momentum so the cooling dynamics will be slow and simulation should be run for relatively long times which makes stochastic differential equation solvers to be numerically unstable. Then the case with stochastic noise will be studied with relatively low initial momentum.

For the no noise case initial conditions has chosen as $\mathbf{u_0} = (0, 0, p_{x_0}, p_{y_0}, 0, 0)$ where $p_{i_0} = [10, -10]\,\hbar k$. In addition, due to absence of stochastic momentum noise corresponding to momentum kicks due to spontaneous photon emissions, the particle will be cooled down to zero kinetic energy in corresponding direction.

As it can be seen from Fig. 5 in non-rotating case momentum in y direction making a simple harmonic motion due to harmonic potential. Nevertheless, in the rotating case due to coupling between x and y directions both momentum has cooled down and particle has trapped in both direction.

As it can be seen from Fig. 6 due to coupling between x and y direction transverse direction has cooled down in presence of rotation as in the previous figure.

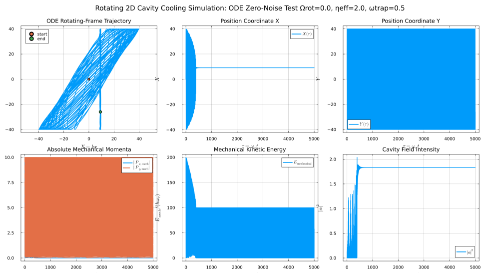

(a) $\Omega_{\text{rot}} = 0\omega_r$

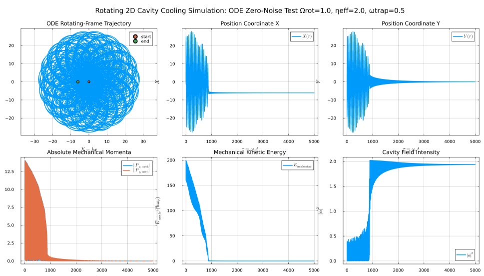

(b) $\Omega_{\text{rot}} = 1.0\omega_r$

FIG. 5. Semiclassical zero-noise ODE dynamics for the initial condition $(P_{x0}, P_{y0}) = (10, 10)$. All other parameters are chosen as in Eq. (83).

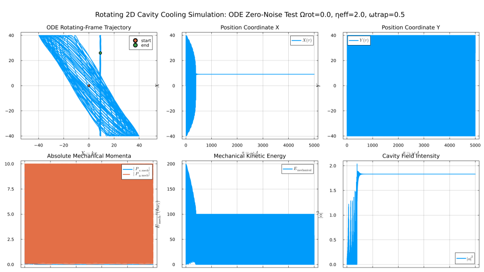

(a) $\Omega_{\text{rot}} = 0\omega_r$

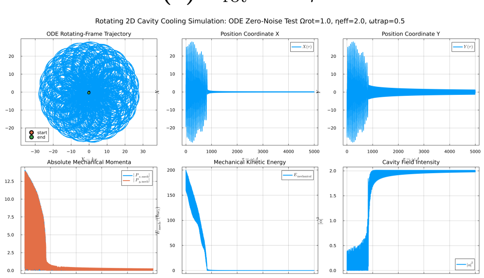

(b) $\Omega_{\text{rot}} = 1.0\omega_r$

FIG. 6. Semiclassical zero-noise ODE dynamics for the initial condition $(P_{x0}, P_{y0}) = (10, -10)$. All other parameters are chosen as in Eq. (83).

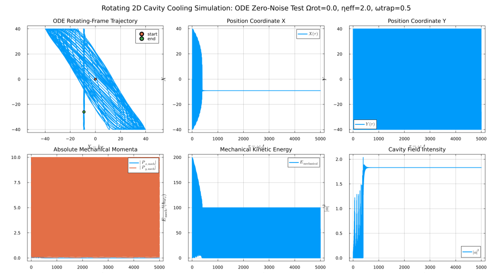

(a) $\Omega_{\text{rot}} = 0\omega_r$

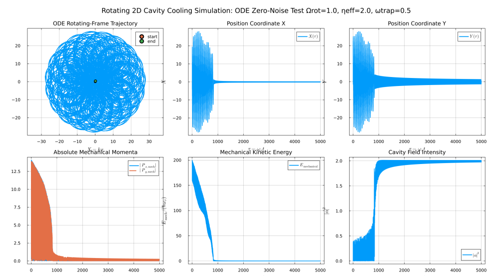

(b) $\Omega_{\text{rot}} = 1.0\omega_r$

FIG. 7. Semiclassical zero-noise ODE dynamics for the initial condition $(P_{x0}, P_{y0}) = (-10, 10)$. All other parameters are chosen as in Eq. (83).

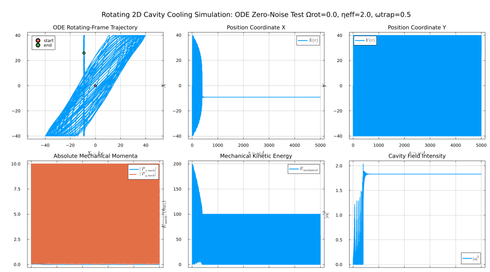

(a) $\Omega_{\text{rot}} = 0\omega_r$

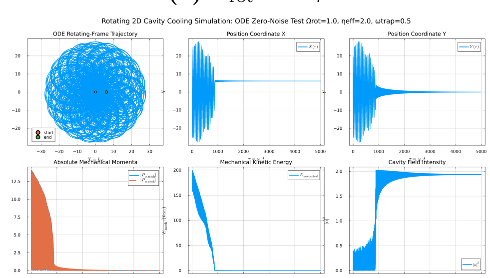

(b) $\Omega_{\text{rot}} = 1.0\omega_r$

FIG. 8. Semiclassical zero-noise ODE dynamics for the initial condition $(P_{x0}, P_{y0}) = (-10, -10)$. All other parameters are chosen as in Eq. (83).

As we can observe from Figs. 5, 6, and 7; lower intensity steady state of the system in rotating case has acquired when the particle trapped at nonzero x. In addition, more efficient cooling has observed when the particle trapped again at nonzero x.

As it can be seen from Fig. 8, observations acquired from previous figures are valid for this figure also. In addition, due to additional trapping-like potential coming from vector potential in presence of rotation the particle has trapped closer to origin in x direction compared to non-rotating case.

To check the stability of $x = 0$ steady state we will put the particle at $x_0 = 0$ with small initial kick to observe the solution. Since the Jacobian stability analysis gives inconclusive results for $x = 0$ at non-rotating case we can just test it in simulation.

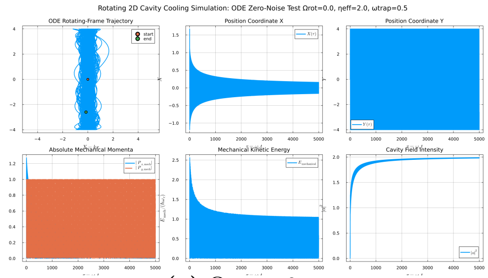

(a) $\Omega_{\text{rot}} = 0\omega_r$

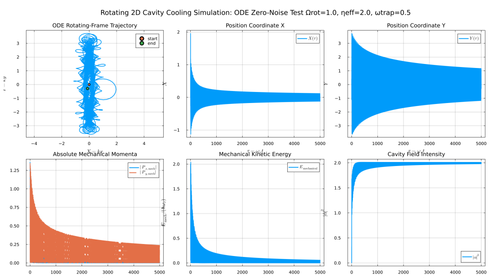

(b) $\Omega_{\text{rot}} = 1.0\omega_r$

FIG. 9. Semiclassical zero-noise ODE dynamics for the initial condition $(P_{x0}, P_{y0}) = (1, 1)$. All other parameters are chosen as in Eq. (83).

As it can be seen from Fig. 9 starting with smaller initial momentum had slowed the time dynamics but we can see that $x = 0$ is a stable steady state for both rotating and non-rotating case since the particle trapped at 0 along x direction. One can also capture other steady states found in Figs. 10 and 11 by altering the initial conditions.

Plot Note 1 - SDE plots will be added.

Plot Idea 1 - p_x and p_y plots can be separated to distinguish the differences better.

Plot Idea 2 - A color gradient on trajectory line can be added $x - y$ trajectory to observe the time evolution of the trajectory of particle.

C. Stationary State Analysis for Semiclassical Approach

To find the steady state of the reduced system we need to make the assumptions of $y = y_{\text{fix}}$ and $p_y = p_{y\text{fix}}$. It is sensible to choose $y_{\text{fix}} = 0$ here since only extrema of the optical potential along y axis is at $y = 0$. Nevertheless, $p_{y\text{fix}}$ is the canonical momenta which depends on x_{ss}. Unfortunately this condition makes it harder to assign a value and for each x_{ss}, $p_{y\text{fix}}$ will have a different value.

To solve this problem we can run our ODE simulation and use the resulting $p_{y\text{fix}}$ value in Eq. (72). Furthermore, we can investigate the results of root finding algorithm to find matching x_{ss} in the outcome of ODE simulation to compare $|\alpha|^2_{\text{ss}}$.In addition, one can also observe the behavior of steady state quantity with the changing Ω_{rot}.

Initially, we can assume $p_{y\text{fix}} = 0$ to investigate the behavior of quantity of steady states. Different values of $p_{y\text{fix}}$ shifts the linear part of Eq. (72) along x axis so one can argue that it does not alter the number of solutions greatly since the nonlinear part is periodic but changes the value of the solutions and the symmetry between negative and positive x_{ss} in terms of number of solutions. this symmetry argument will be clear with the following figures. The parameters will be the same as in Eq. (83).

Solutions for x_{ss} and $|\alpha|^2_{\text{ss}}$ will be given for $p_{y\text{fix}} = 0$ along with $p_{y\text{fix}} = \pm 1\hbar k$ to clarify the symmetry changing argument.

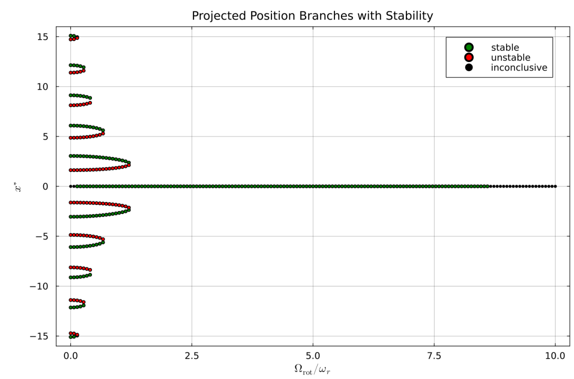

FIG. 10. Projected position branches with stability for $p_{y\text{fix}} = 0$.

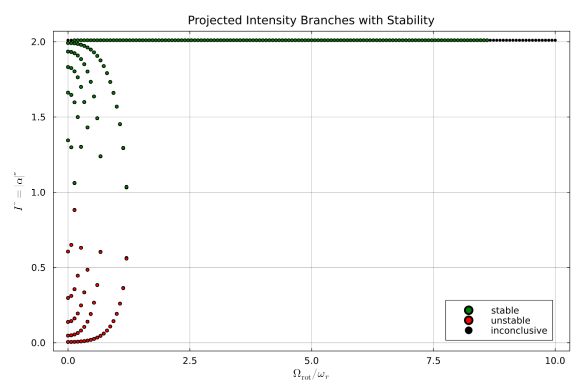

FIG. 11. Projected intensity branches with stability for $p_{y\text{fix}} = 0$.

As it can be seen from Figs. 11 and 10 number of steady states of the reduced system is decreasing with the increasing Ω_{rot} since it also increase the analogous trapping potential deriving from vector potential and after one point only solution for x is $x_{\text{ss}} = 0$ again due to increasing trapping. In addition, one can observe that for $\Omega_{\text{rot}} = 0$, stability of $x_{\text{ss}} = 0$ inconclusive with Jacobian analysis. We can see that the highest intensity steady state corresponds to $x_{\text{ss}} = 0$ as we claimed if we consider Fig. 12.

As it can be seen from Fig. 12, steady state intensity is decreasing as the distance between origin and point which particle has trapped increasing. Furthermore, This difference gets between intensity steady states gets larger as

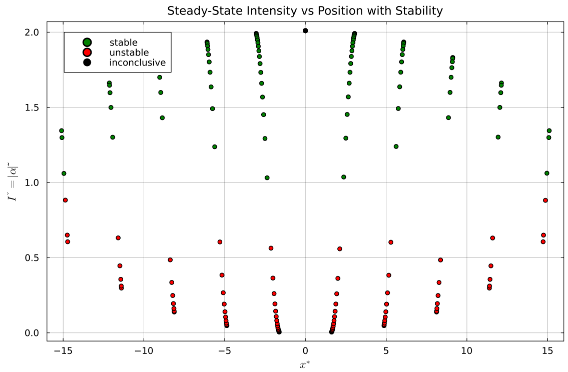

FIG. 12. Steady-state intensity versus position with stability for $p_{y\text{fix}} = 0$.

we increase Ω_{rot}. In addition, relatively low intensity solutions are unstable since x_{ss} they correspond are sitting on unstable points of the optical potential. In addition the Jacobian analysis gives inconclusive result for $x_{\text{ss}} = 0$ when there is no rotation in the system but we can conclude that it is stable since we can capture it in ODE simulation result provided in Fig. 9.

Now if we consider $p_{y\text{fix}} = \pm 1\hbar k$ cases the symmetry argument will be more clear.

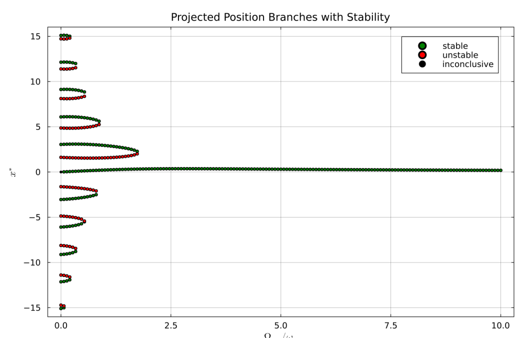

(a) $p_{y\text{fix}} = 1$

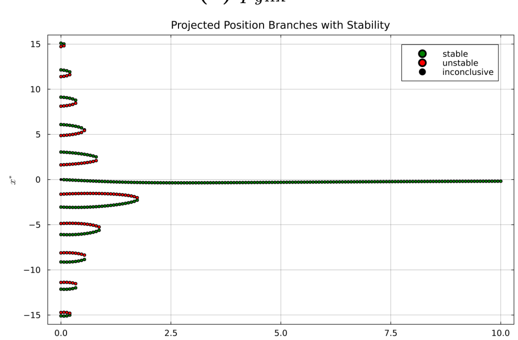

(b) $p_{y\text{fix}} = -1$

FIG. 13. Projected position branches with stability for $p_{y\text{fix}} = 1$ and $p_{y\text{fix}} = -1$.

As it can be seen from Fig. 13 due to sign of $p_{y\text{fix}}$, number of steady states for $x < 0$ and $x > 0$ is different for certain values of Ω_{rot} but the overall phenomena of decreasing number of steady states with increasing Ω_{rot} can be observed for asymmetric case too.

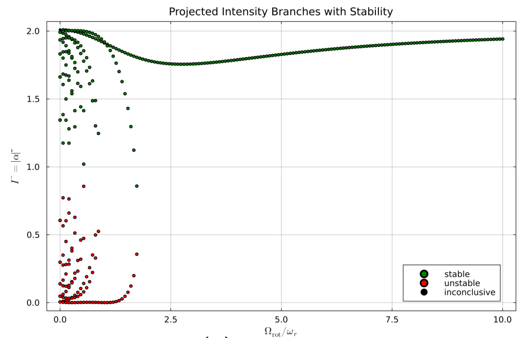

(a) $p_{y\text{fix}} = 1$

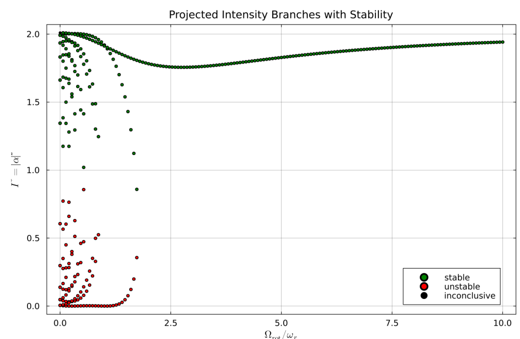

(b) $p_{y\text{fix}} = -1$

FIG. 14. Projected intensity branches with stability for $p_{y\text{fix}} = 1$ and $p_{y\text{fix}} = -1$.

Fig. 14 shows that the number of steady states has increased for some values of Ω_{rot} compared to symmetric case but there is no explicit dependence on the sign of $p_{y\text{fix}}$ for intensity. The difference comes from the corresponding values of x_{ss} for intensity steady states.

The Fig. 15 also depicts that the symmetry around $x = 0$ has broken due to nonzero $p_{y\text{fix}}$ but the points corresponding $\Omega_{\text{rot}} = 0$ case has not changed since $p_{y\text{fix}}$ term vanishes from Eq. (72) when $\Omega_{\text{rot}} = 0$.

Now we can explicitly investigate the steady states for distinct values of Ω_{rot} by finding and substituting the correct value of $p_{y\text{fix}}$ into Eq. (72).

Since $p_{y\text{fix}}$ does not have any effect on steady states when $\Omega_{\text{rot}} = 0$, Fig. 16 shows the accurate steady states of the non-rotating case. We captured some of the distinct steady states in Figs. 5, 7, and 9. Nevertheless, for the rotating case the calculations becomes tricky if we want accurate results.

We first run the simulation to determine the values of $p_{y\text{fix}}$ corresponding to each steady state. Then substituting the value obtained from the simulation to Eq. (72) we expect to get accurate results for rotating case also.

For the steady state, $x_{\text{ss}} = 0$, in rotating case presented in Figs. 6, 7, and 9; $p_{y\text{fix}} = 0$ has reached from the result of simulation. Then by substitution the steady states of the system for $\Omega_{\text{rot}} = 1$ and $p_{y\text{fix}} = 0$ found from Eqs. (72) and (73) are,

We can compare the corresponding intensity for $x_{\text{ss}} = 0$, depicted as 3, in Fig. 17 to steady state reached in

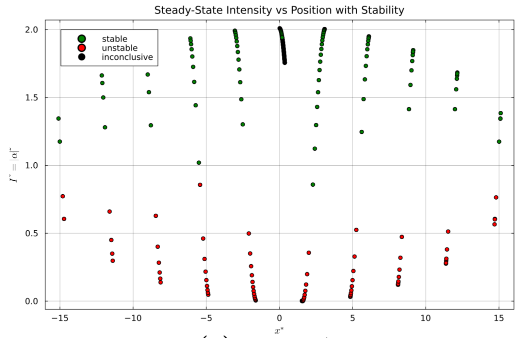

(a) $p_{y\text{fix}} = 1$

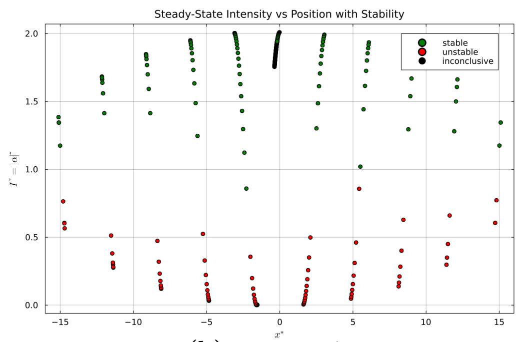

(b) $p_{y\text{fix}} = -1$

FIG. 15. Steady-state intensity versus position with stability for $p_{y\text{fix}} = 1$ and $p_{y\text{fix}} = -1$.

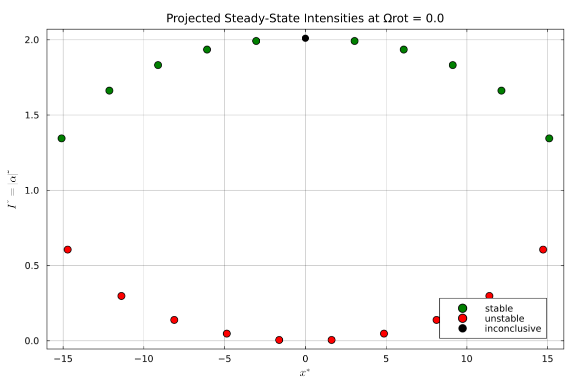

FIG. 16. Steady states with stability for $\Omega_{\text{rot}} = 0$.

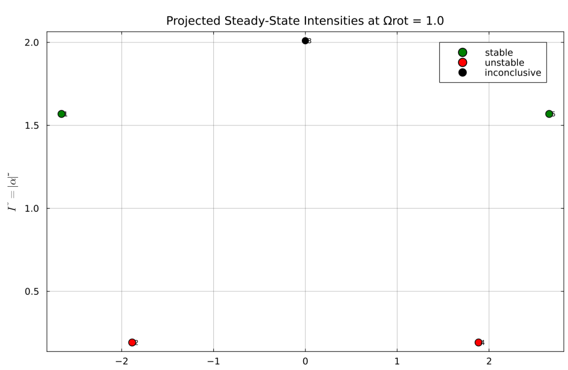

FIG. 17. Steady states with stability for $\Omega_{\text{rot}} = 1$ and $p_{y\text{fix}} = 0$.

Figs. 6, 7, and 9. As it can be observed from mentioned figures the the result is accurate for the corresponding $x_{\text{ss}} = 0$.

For the steady state, $x_{\text{ss}} = -6.08897$, in rotating case presented in Fig. 5, $p_{y\text{fix}} = -3.04451$ has reached from the result of simulation. Then by substitution the steady states of the system for $\Omega_{\text{rot}} = 1$ and $p_{y\text{fix}} = -3.04451$ found from Eqs. (72) and (73) are,

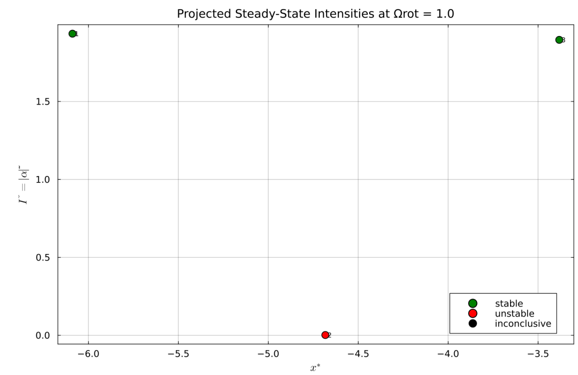

FIG. 18. Steady states with stability for $\Omega_{\text{rot}} = 1$ and $p_{y\text{fix}} = -3.04451$.

We can compare the corresponding intensity for $x_{\text{ss}} = -6.08897$, depicted as 1, in Fig. 18 to steady state reached in Fig. 5. As it can be observed from mentioned figures the the result is accurate for corresponding $x_{\text{ss}} = -6.08897$. In addition we can also observe the decrease in steady state intensity between Figs. 17 and 18 exactly as we observed between Figs. 6 and 5.

For the steady state, $x_{\text{ss}} = 6.08897$, in rotating case presented in Fig. 8, $p_{y\text{fix}} = 3.04451$ has reached from the result of simulation. Then by substitution the steady states of the system for $\Omega_{\text{rot}} = 1$ and $p_{y\text{fix}} = 3.04451$ found from Eqs. (72) and (73) are,

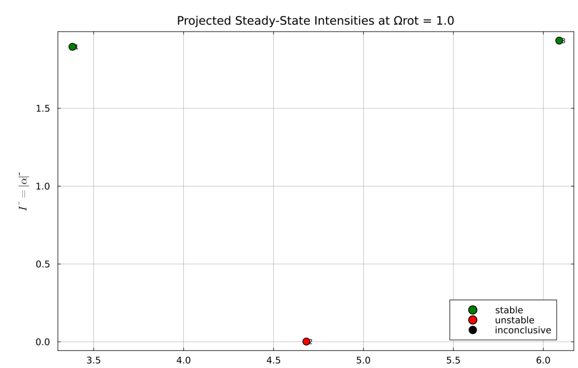

FIG. 19. Steady states with stability for $\Omega_{\text{rot}} = 1$ and $p_{y\text{fix}} = 3.04451$.

We can compare the corresponding intensity for $x_{\text{ss}} = 6.08897$, depicted as 3, in Fig. 19 to steady state reached in Fig. 8. As it can be observed from mentioned figures the the result is accurate for corresponding $x_{\text{ss}} = 6.08897$.

In addition we can also observe the decrease in steady state intensity between Figs. 17 and 19 exactly as we observed between Figs. 6 and 8.

Plot Idea 1 - Instead of directly using green,black and red we can use a color gradient corresponding to value of the real part of eigenvalue of the Jacobian so that we can observe how dynamics changes with the changing rotation for different steady states.